American Journal of
Biomedical Science & Research

www.biomedgrid.com
ISSN: 2642-1747

Research Article

Examining the Antibacterial Activity of Cerium Oxide, Zinc Doped Cerium Oxide for *E. Coli* and *S. Auerus*

Rehana Riaz* and Syed Ahmed Shuja

Department of Physics, International Islamic University, Islamabad, Pakistan

***Corresponding author:** Rehana Riaz, Department of Physics, International Islamic University, Islamabad, Pakistan.

To Cite This Article: *Rehana Riaz* and Syed Ahmed Shuja. Examining the Antibacterial Activity of Cerium Oxide, Zinc Doped Cerium Oxide for E. Coli and S. Auerus. Am J Biomed Sci & Res. 2024 25(2) AJBSR.MS.ID.003294,* DOI: 10.34297/AJBSR.2024.25.003294

Received: December 12, 2024; **Published:** December 16, 2024

Abstract

This research focuses on combating bacterial infections by synthesizing cerium oxide (CeO2) and modifying it with 2% and 5% zinc doping, along with 1% graphitic carbon, using the sol-gel method. Structural, morphological, optical, and antibacterial properties were systematically investigated. X-Ray Diffraction (XRD) revealed an increase in crystallite size from 12nm for pure cerium oxide to 26nm for 5% zinc-doped cerium oxide after annealing. Scanning Electron Microscopy (SEM) confirmed agglomerated spheroidal structures for all samples. Diffuse Reflectance Spectroscopy (DRS) showed a widened energy band gap, from 3.15eV for pristine cerium oxide to 3.31eV for the annealed 5% zinc-doped cerium oxide, suggesting potential alterations in electronic properties. Antibacterial activity demonstrated that 1% graphitic carbon- modified cerium oxide exhibited the maximum zone of inhibition against Escherichia coli and Staphylococcus aureus, indicating superior antibacterial activity compared to other synthesized materials. Thus, this study showcases a tailored approach to cerium oxide nanoparticles, highlighting the significance of modifications for enhanced antibacterial applications. The findings in this research contribute to the development of advanced antibacterial agents, leveraging the unique properties of modified cerium oxide nanoparticles.

Keywords: Antibacterial activity, Cerium oxide, Sol-gel, *E. coli*, *S. aurus*

Introduction

Bacterial infections significantly affect public health, posing significant medical problems such as septicaemia, sepsis, cellulitis, and mortality threats [1]. These medical issues can be prevented by taking antibiotics that assist the body in combating bacteria [2]. Recent advancements in nanotechnology have improved the treatment and proliferation of bacterial and microbial infections. However, nanotechnology in medicine offers innovative treatments that effectively address drug resistance, especially in cases where antibiotics are no longer effective against bacterial infections [3,4]. Nanoparticles are receiving significant interest as innovative anti-bacterial agents due to their high surface area-to- volume ratio and distinctive physical and chemical characteristics [5]. Over 1814 nanoparticle-enabled medication have been produced, primarily consisting of metal and metal oxides [6].

Metal and metal oxide nanoparticles, such as gold, nickel, silver, iron, carbon, zinc, cerium, etc., are increasingly attracting attention due to their ability to selectively block metabolic pathways, interact with bactericidal activity, and eliminate bacteria that are resistant to several drugs [7-12]. Cerium oxide (CeO_2) has gained significant attention as antibacterial agents due to their lower or non-existent toxicity to mammalian cells, in contrast to other nano materials [13-15]. CeO_2 has antibacterial properties without requiring external stimulation, as demonstrated in previous studies [16-18]. Cerium is a rare earth metal and the initial element in the lanthanide series on the periodic table. Cerium is unique among rare earth metals as it may be found in both the 3^+ and 4^+ oxidation states.

Cerium oxide, or ceria, is a cubic fluorite-type oxide with Cerium ions at the face and vertices, and oxygen ions at the tetrahedral vacancies of the cubic unit cell [19,20]. Cerium oxide is a focus of research in nanotechnology because of its unique qualities such as low toxicity, high stability, ductility, chemical reactivity, and strong oxidation catalytic capabilities, with potential for catalytic anti

oxidation [21-24]. Various methods have been found in the literature for producing nanostructures include hydrothermal, sol-gel, co-precipitation, and laser ablation [25-28].

In the present research, sol-gel synthesis is chosen for its cost-effectiveness and proven antibacterial properties documented in literature [29,30]. This research investigated the antibacterial properties of *E. coli* and S. aureus. *E. coli* is a gram-negative bacterium that causes diarrheal sickness, whereas S. aureus is a gram-positive bacterium associated with skin and tissue infections. Recent research has shown that cerium oxide is effective in fighting these two bacteria [31-34]. Zinc oxide is of great interest because of their low toxicity, which makes them helpful in other sectors, such as biomedicine. Zinc is doped with cerium oxide to improve its characteristics due to its demonstrated ability to inhibit both microorganisms [35,36]. Research conducted by *S. Jairam, et al*. demonstrated that cerium oxide doped with 8% zinc possesses strong antibacterial properties against S. mutans. expanding on this finding, a study has been carried out using varying concentrations of zinc (0%, 2%, and 5%) and 1% graphitic carbon doped with cerium oxide annealed at 900˚C to test its effectiveness against *E. coli* and S. aureus [37].

Experimental Section

Materials

For the synthesis of cerium oxide (CeO_2) and Zn:CeO_2, anhydrous cerium chloride ($CeCl_3$) and zinc chloride ($ZnCl_2$) were employed as precursor agents. As a solvent, distilled water (H_2O) was utilized. Gel formation was facilitated by the utilization of sodium hydroxide (NaOH). Isopropanol alcohol (C_3H_8O) and nitric acid (HNO_3) were employed to aid in the chemical synthesis. *E. coli* and *S. auerus* are utilized as a bacterium to evaluate the antibacterial effects of the prepared samples. For the antibacterial analysis, Graphitic Oxide (GO) ceria has also been prepared from graphite powder. All of these materials were purchased from the company Sigma Aldrish.

Synthesis

A solution of sol can be obtained by combining a 2M (molar) solution of NaOH with 1M solution of $CeCl_3$ and agitating continuously at 80˚C for 60minutes using a magnetic stirrer. As diluting solvents, five droplets of HNO_3 and C_3H_8O were added to the prepared solution. By combining distilled water with 2%, 5% $ZnCl_2$ and 1% (GO), an additional solution of Zn^{+2} ions was produced. An additional CeO_2 solution was supplemented drop by drop with this $ZnCl_2.6H_2O$ solution and graphite oxide solution. After 25minutes of agitating and heating, the two solutions were centrifuged at 2500rpm for an additional 35minutes. Throughout the synthesis of cerium oxide, the subsequent reaction occurred with the phase transition from CeOCl to CeO_2:

$$CeCl_3 + NaOH \rightarrow CeOCl + NaCl + HCl \quad (1)$$

$$CeOCl + 2HCl + O_2 \rightarrow CeO_2 + 2H_2O + 2Cl_2 \quad (2)$$

The solutions were allowed to sediment for thirty minutes and were rinsed three times to remove any contaminants and placed in furnace at 900˚C. The dip-coating approach was used to deposit thin films of cerium (IV) oxide, (2% and 5%) zinc doped cerium oxide and graphitic carbon cerium oxide onto a glass substrate.

Antibacterial

The nanostructures were evaluated for their antibacterial efficacy against Escherichia coli (*E. coli*) and Staphylococcus aureus (S. aureus) obtained from the Centre for Interdisciplinary Research in Basic Science (CIRBS). Methyl sulphur oxide served as the positive control. Bacteria were grown in a nutrient fluid medium at room temperature on a furnace operating at 2500rpm. Following the Optical Density (OD) test, bacteria were diluted in a fluid and transferred to 250-well plates. Fifteen nanoliters of methyl sulphur oxide solution was added to each plate. We measured the diameter of the living area to assess the antibacterial effectiveness of the manufactured nanostructures. The antibacterial mechanism targets the outer coats of bacteria, specifically peptidoglycan and lipopolysaccharide, which protect them from external chemical agents [38]. The nanostructures interact with the bacterium's outer layer through two mechanisms. The outer layer of bacteria can absorb it in the form of ions by electrostatic forces, specifically ionic forces [39]. Another process involves oxidation-reduction, in which the Ce^{+4} charge is converted to Ce^{+3} by bacteria, causing oxidative stress in the microorganism's outer membrane and limiting its bacterial effects [40,41].

Characterization

Using an X-ray diffractometer (XPERT-3 with Cu (copper) K_α radiations), structural analysis was performed on as-prepared samples of thin films deposited on a glass substrate. The apparatus was equipped with a wavelength of 1.540589Å and operated at a voltage of 40kV and an applied current of 40mA. The morphology of nanostructures was analyzed using scanning electron microscopy (JSM-6490) with an accelerating voltage of 20kV. The optical characteristics were analyzed utilizing a spectrometer system. Data analysis and plotting for XRD and DRS results were performed utilizing Microsoft Excel and Origin Lab software.

Results and Discussions

Structural Characterization

X-ray diffraction (XRD) analysis was conducted in order to gain a deeper comprehension of the crystal structure and phase purity of cerium oxide, un annealed zinc doped cerium oxide and annealed zinc doped cerium oxide. (Figure 1) presents the X-ray diffraction (XRD) diffractogram patterns of the un annealed and samples subjected to annealing, at a temperature of 900˚C. The patterns revealed consistent alignment of all peaks to the standard data (JCPDS, 34-0394) of a cubic fluorite structure of CeO_2. The findings indicate a strong correlation between the diffraction patterns and the indexing of the face centered cubic fluorite structure of CeO_2 with respect to the planes (111), (200), (220), (311), (331). Nevertheless, it is apparent that all precursor elements underwent com-

plete decomposition, as indicated by (Figure 1) corresponding to the structure of cerium oxide (Figure 1).

Nanostructures of all samples have (111) orientation as the peak exhibits the highest intensity and indicates a favored growth plane. The diffractogram patterns of zinc doped cerium oxide samples do not exhibit any discernible peak that suggests the presence of zinc or its derivatives, hence confirming the purity of zinc doped cerium oxide. However, the absence of any peak of Zn in the XRD pattern confirmed that the dopant concentration of x=0.02 and 0.05 is within the solid solubility limit as confirmed by the prior literature too [42]. Nevertheless, notable alterations were observed in the majority of the peaks. The mean size has the CeO_2 nanoparticles has been estimated from full width at half maximum (FWHM) and Debye-Sherrer formula according to equation the following:

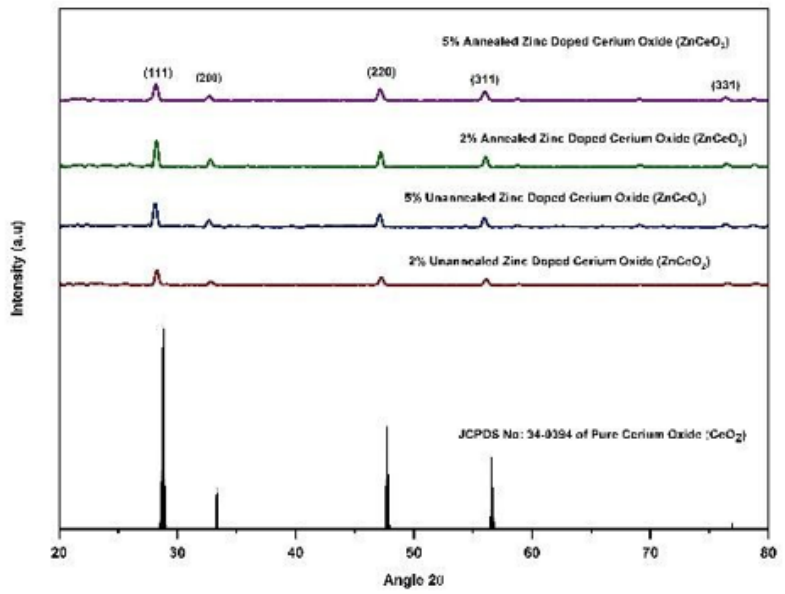

Figure1: XRD spectrum of all the samples.

$$D = \frac{k\lambda}{\beta \cos\theta} \quad (3)$$

where, 0.89 is the shape factor, λ is the X-ray wavelength, β is the line broadening at half the maximum intensity (FWHM) in radians, and θ is the Bragg angle. The mean size of annealed CeO_2 nanoparticles was determined around 20nm. It was observed that as zinc was incorporated in cerium oxide it increases the crystal size for the samples gradually i.e., for un annealed cerium oxide the approximate particle size is 12nm nm which increases 22nm for $Zn_{0.02}Ce_{0.98}O_2$ and 23nm for to $Zn_{0.05}Ce_{0.95}O_2$. A previous literature confirms this as it explained that Zn^{+2} (90pm) occupying interstitial lattice sites, which causes the lattice to expand when incorporated in Ce^{+4} (97pm) lattice [43]. Similar results are observed for annealed samples of $Zn_{0.02}Ce_{0.98}O_2$ and $Zn_{0.05}Ce_{0.95}O_2$ as size shifted to 24nm and 26nm respectively.

Moreover, it was observed in (Figure 1) that as the zinc concentration increases intensities of the diffraction peaks exhibited an upward trend as well as the lattice parameter. However, there was an overall decrease in comparison to pure cerium oxide. This observation suggests that a higher annealing temperature supplies ample energy for the crystallization process to occur, resulting in the proper orientation of crystals at equilibrium sites and leading to an increase in intensity. Several other parameters were calculated in (Table 1) for all the samples.

Table 1: Calculated parameters for all the samples.

Sample Name	Lattice Parameter a (Å)	Crystallite Size D (nm)	Dislocation Density $\delta \times 10^5 (m^{-2})$	Micro Strain (Ɛ)
CeO_2	5.41	12	2.36	0.0017
$Zn_{0.02}Ce_{0.98}O_2$	3.48	22	2.06	0.0016
$Zn_{0.05}Ce_{0.98}O_2$	4.01	23	1.84	0.0015
Annealed $Zn_{0.02}Ce_{0.98}O_2$	3.22	24	1.71	0.0014
Annealed $Zn_{0.02}Ce_{0.98}O_2$	3.22	26	1.45	0.0013

SEM

Scanning electron microscopy was used to conduct morphological examination. (Figure 2) (a, b, c, d, e) displays the physical structure of pure cerium oxide, un annealed $Zn_{0.02}CeO_2$, annealed $Zn_{0.02}Ce_{0.98}O_2$, unannealed $Zn_{0.05}Ce_{0.95}O_2$ and annealed $Zn_{0.05}Ce_{0.95}O_2$ at temperature of 900˚C respectively. The morphological study of the Zn doped cerium nanoparticles revealed some clustered cubic nanoparticles for both un annealed samples. Similar results were also observed in prior literature [44]. The morphology of pure cerium oxide and annealed samples of zinc doped cerium oxide was observed as agglomeration of small crystallites as at higher temperature, small crystallites are clinging together to form a large agglomerated spheroidal structure [45]. This confirms the fact that structures obtained specific shapes when subjected to temperature (Figure 2).

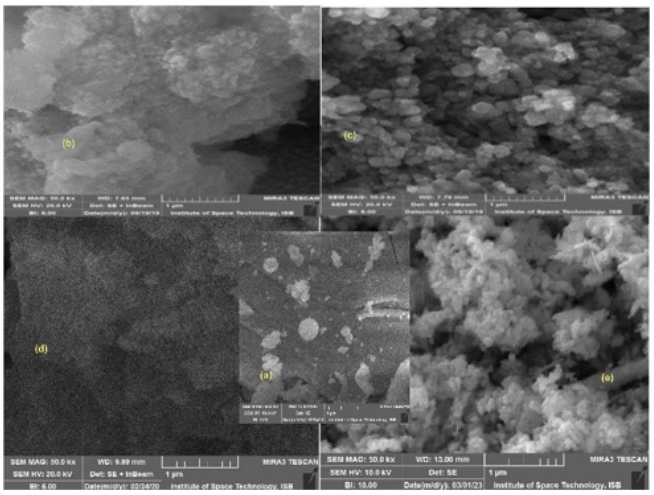

Figure 2: SEM images of (a, b, c, d, e) pure cerium oxide, un annealed $Zn_{0.02}CeO_2$, annealed $Zn_{0.02}CeO_2$, unannealed $Zn_{0.05}Ce0.98O_2$ and annealed $Zn_{0.05}CeO_2$ at temperature of 900˚C respectively.

DRS

The optical absorption spectra for samples of pure CeO_2, annealed and un annealed $Zn_{0.02}Ce_{0.98}O_2$ and $Zn_{0.05}Ce_{0.95}O_2$ in the wavelength range of 200nm - 800nm are shown in figure, and figure shows the optical band gap of all the samples at room temperature using Tauc's plot. The optical band gap is shown by the extra plot of the straight line in figure. Optical properties of all the prepared samples have been studied using UV-VIS Spectrophotometer (SHIMADZU 2700) (Figure 3).

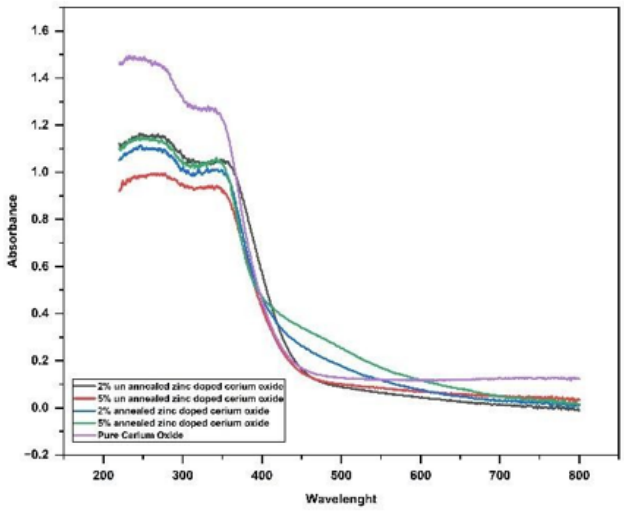

Figure 3: Absorption spectra of all the samples.

The maximum absorption peaks of the samples were observed at wavelengths of 240nm, 250nm and 260nm, 250nm and 280nm for pure cerium oxide, un annealed $Zn_{0.02}Ce_{0.98}O_2$, un annealed $Zn_{0.05}Ce_{0.95}O_2$, annealed $Zn_{0.02}Ce_{0.98}O_2$ and annealed $Zn_{0.05}Ce_{0.95}O_2$ respectively. The slight shift in absorption peaks of Zn doped CeO_2 are due to exchange interaction of d-f and d electrons of Zn^{2+} ions [46]. The pure cerium oxide showed improved absorbance in the 200nm - 500nm range as compared to all other nanoparticles sample.

We have,

$$\alpha hv\,\alpha(hv-E_g)^n \quad (4)$$

where,

$$hv=\frac{1240(evXnm)}{\lambda(nm)} \quad (5)$$

and,

$$\alpha=\frac{2.302A}{d} \quad (6)$$

α represents the absorption coefficient, A represents the absorbance, and d represents the thickness taken as unity. To determine the direct optical band (allowed transition), a graph is generated plotting $(\alpha hv)^2$ against energy (hv). It is observed that the band gap of CeO_2 nanocrystals is 3.15eV and this value increased to 3.17eV ($Zn_{0.02}Ce_{0.98}O_2$) and 3.25eV ($Zn_{0.05}Ce_{0.95}O_2$) for Zn doped samples. The band-edge absorption of nanoscale semiconductor materials is mainly dependent on two factors: the quantum size and interface effects. Generally, the quantum size effect leads to a blue shift that predicts an increase of the band-gap value, while the interface effects induce a red shift. In this work, the quantum size effect should be responsible for the variation of the absorption band edge [47]. After undergoing annealing at a temperature of 900˚C, the optical characteristics undergo a shift in trend, resulting in a band gap of 3.24eV and 3.31eV for $Zn_{0.02}Ce_{0.98}O_2$ and $Zn_{0.05}Ce_{0.95}O_2$ respectively. This change can be attributed to the increase in crystallite size and alterations in morphology caused by heating (Figure 4).

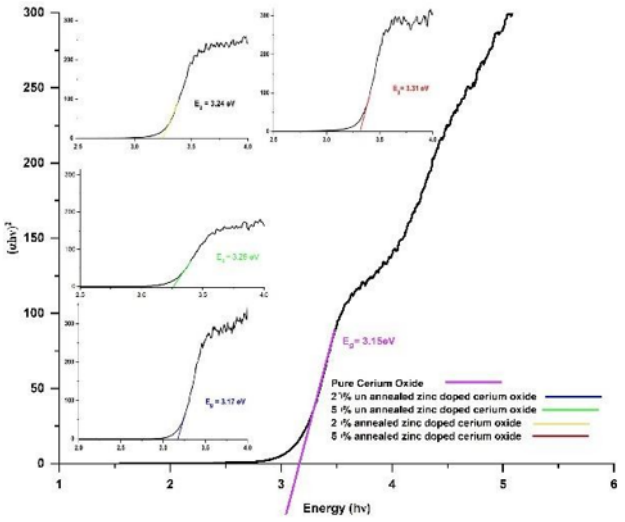

Figure 4: Band gaps of all the samples.

Anti-Bacterial Activity

To evaluate the antimicrobial activity of synthesized different combinations, a disc diffusion method was performed against the resistant strain of *E. coli* and *S. aureus* (Figure 5) (Figure 6).

In the present study five compounds were studied the order of which is represented in the (Table 2) below. Sample 6 is a baseline according to which we can compare the effectiveness of other samples. From the result of antibacterial activity, it is clear that all the samples show better results of CeO_2 nano composites. For gram positive, $Zn_{0.05}Ce_{0.95}O_2$ has significant inhibition efficiency for S. Aureus (B). However, in case of gram-negative sample i.e., *E. coli* (A) graphitic carbon is high antibacterial element as compared to zinc doped cerium oxide as its zone of inhibition is 28mm approximately from measurements (Table 2).

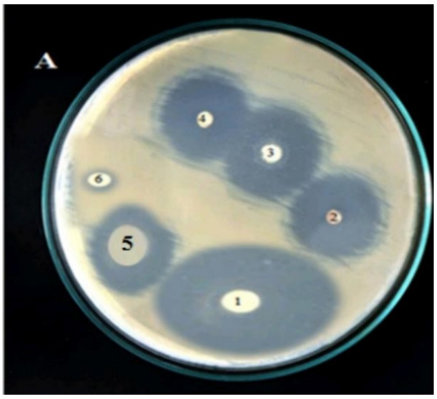

Figure 5: Antibacterial activity of all the samples for *E. coli*.

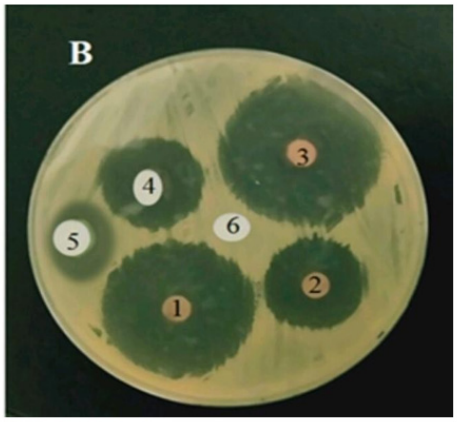

Figure 6: Antibacterial activity of all the samples for *S. auerus*.

Table 2

Samples Numbers	Sample Code	Zone of Inhibition (mm)	
		Gram Positive	Gram Negative
		S. Aureus	*E. Coli*
Sample 1	$GO+Zn_{0.05}Ce_{0.95}O_2$	22	28
Sample 2	$Zn_{0.05}Ce_{0.95}O_2$	15	16
Sample 3	$GO+Zn_{0.02}Ce_{0.98}O_2$	23	17
Sample 4	$Zn_{0.02}Ce_{0.92}O_2$	14	15
Sample 5	CeO_2	9	13
Sample 6	Standard		

Conclusion

In conclusion, the sol-gel synthesis and modification of cerium oxide nanoparticles, incorporating zinc doping (2% and 5%) and 1% graphitic carbon, exhibit promise in the treatment of bacterial infections. The increased crystallite size, particularly in 5% zinc- doped cerium oxide post-annealing, signifies structural improvements for enhanced stability. Scanning electron microscopy confirms non uniform agglomerated spheroidal structures. Diffuse reflectance spectroscopy indicates shifts in the energy band gap, influencing optical properties. Antibacterial assessments highlight the superior efficacy of 1% graphitic carbon-modified cerium oxide, emphasizing its potential in augmenting antibacterial properties. These findings underscore the potential of tailored cerium oxide nanoparticles for advanced antibacterial applications, warranting further exploration in this dynamic field.

Authors Contribution

Rehana Riaz contributed to the conception design and drafting of the manuscript, analysis of the study was done by Hira Sarfraz.

Competing Interests

The author(s) have no competing interests.

Acknowledgement

None.

References

1. Doron S, SL Gorbach (2008) Bacterial infections: overview. International Encyclopedia of Public Health: 273-282.
2. Roberts CA, JE Buikstra (2019) Bacterial infections, in Ortner's Identification of pathological conditions in human skeletal remains. Elsevier: 321-439.
3. Ahmadi Shadmehri A, F Namvar (2020) A review on green synthesis, cytotoxicity mechanism and antibacterial activity of Zno-NPs. Journal of Research in Applied and Basic Medical Sciences 6(1): 23-31.
4. Helal F Hetta, Yasmin N Ramadan, Alhanouf I Al Harbi, Esraa A Ahmed, Basem Battah, et al. (2023) Nanotechnology as a promising approach to combat multidrug resistant bacteria: a comprehensive review and future perspectives. Biomedicines 11(2): 413.
5. Shaheen TI, AA Abd El Aty (2018) In-situ green myco-synthesis of silver nanoparticles onto cotton fabrics for broad spectrum antimicrobial activity. International Journal of Biological Macromolecules 118: 2121-2130.
6. Xiaomei Liu, Jingchun Tang, Lan Wang, John P Giesy (2018) Mechanisms of oxidative stress caused by CuO nanoparticles to membranes of the bacterium Streptomyces coelicolor M145. Ecotoxicology and environmental safety 158: 123-130.
7. Getie s, Abebe Belay Gemta, Chandra Reddy AR, Zerihun Belay (2017) Synthesis and characterizations of zinc oxide nanoparticles for antibacterial applications. J Nanomed Nanotechno 8(004).
8. Qi Xin, Hameed Shah, Asmat Nawaz, Wenjing Xie, Muhammad Zain Akram, et al. (2019) Antibacterial carbon-based nanomaterials. Advanced Materials 31(45): e1804838.
9. Saddam Saqib, Muhammad Farooq Hussain Munis, Wajid Zaman, Fazal Ullah, Syed Nasar Shah, et al. (2019) Synthesis, characterization and use of iron oxide nano particles for antibacterial activity. Microscopy research and technique 82(4): 415-420.
10. Ahghari MR, V Soltaninejad, A Maleki (2020) Synthesis of nickel nanoparticles by a green and convenient method as a magnetic mirror with antibacterial activities. Scientific reports 10(1): 12627.
11. Gu X (2021) Preparation and antibacterial properties of gold nanoparticles: A review.
12. Environmental Chemistry Letters 19: 167-187.
13. Karli Gold, Buford Slay, Mark Knackstedt, Akhilesh K Gaharwar (2018) Antimicrobial activity of metal and metal-oxide based nanoparticles. Advanced Therapeutics 1(3): 1700033.
14. Laura De Marzi, Antonina Monaco, Joaquin De Lapuente, David Ramos, Miquel Borras, et al. (2013) Cytotoxicity and genotoxicity of ceria nanoparticles on different cell lines in vitro. International journal of molecular sciences 14(2): 3065-3077.
15. Yi Yang Tsai, Jose Oca Cossio, Kristina Agering, Nicholas Simpson, Mark Atkinson, et al. (2017) Novel synthesis of cerium oxide nanoparticles for free radical scavenging. Nanomedicine 2(3): 325-332.
16. Roy W Tarnuzzer, Jimmie Colon, Swanand Patil, Sudipta Seal (2005) Vacancy engineered ceria nanostructures for protection from radiation-induced cellular damage. Nano letters 5(12): 2573-2577.
17. Jessica T Dahle, Yuji Arai (2015) Environmental geochemistry of cerium: applications and toxicology of cerium oxide nanoparticles. International journal of environmental research and public health 12(2): 1253-1278.
18. Mushtaq A Dar, Rukhsana Gul, Ponmurugan Karuppiah, Naif A Al Dhabi, Assim A Alfadda, et al. (2022) Antibacterial activity of cerium oxide nanoparticles against ESKAPE pathogens. Crystals 12(2): 179.
19. Yashu Kuang, Xiao He, Zhiyong Zhang, Yuanyuan Li, Haifeng Zhang, et al. (2011) Comparison study on the antibacterial activity of nano-or bulk-cerium oxide. Journal of nanoscience and nanotechnology 11(5): 4103-4108.
20. Shin Tsunekawa, Ryoji Sahara, Yoshiyuki Kawazoe, Atsuo Kasuya (2000) Origin of the blue shift in ultraviolet absorption spectra of nanocrystalline CeO2− x particles. Materials transactions JIM 41(8): 1104-1107.
21. Anirban ST Paul, A Dutta (2015) Vacancy mediated ionic conduction in Dy substituted nanoceria: a structure–property correlation study. RSC Advances 5(62): 50186-50195.
22. Ivana Celardo, Jens Z Pedersen, Enrico Traversab, Lina Ghibelli (2011) Pharmacological potential of cerium oxide nanoparticles. Nanoscale 3(4): 1411-1420.
23. MS Yakimova, Vladimir K Ivanov, Olga S Ivanova Polezhaeva, AA Trushin (2009) Oxidation of CO on nanocrystalline ceria promoted by transition metal oxides. Doklady Chemistry 427(2): 186-189.
24. Chen HI, HY Chang (2005) Synthesis and characterization of nanocrystalline cerium oxide powders by two-stage non-isothermal precipitation. Solid state communications 133(9): 593-598.
25. Alessandro Trovarelli, Carla de Leitenburg, Marta Boaro, Giuliano Dolcetti (1999) The utilization of ceria in industrial catalysis. Catalysis today 50(2): 353-367.
26. Myungjoon Kim, Saho Osone, Taesung Kim, Hidenori Higashi, Takafumi Seto, et al. (2017) Synthesis of nanoparticles by laser ablation: A review. KONA Powder and Particle Journal 34: 80-90.
27. Mascolo MC, Y Pei, TA Ring (2013) Room temperature co-precipitation synthesis of magnetite nanoparticles in a large pH window with different bases. Materials 6(12): 5549-5567.
28. Parashar M, VK Shukla, R Singh (2020) Metal oxides nanoparticles via sol–gel method: a review on synthesis, characterization and applications. Journal of Materials Science: Materials in Electronics 31: 3729-3749.
29. Jawwad A Darr, Jingyi Zhang, Neel Makwana, Xiaole Weng (2017) Continuous hydrothermal synthesis of inorganic nanoparticles: applications and future directions. Chemical reviews 117(17): 11125-11238.
30. G Poongodi, P Anandan, R Mohan Kumar, R Jayavel (2015) Studies on visible light photocatalytic and antibacterial activities of nanostructured cobalt doped ZnO thin films prepared by sol–gel spin coating method. Spectrochimica Acta Part A: Molecular and Biomolecular Spectroscopy 148: 237-243.
31. Hyung Jun Jeon, Sung Chul Yi, Seong Geun Oh (2003) Preparation and antibacterial effects of Ag–SiO2 thin films by sol–gel method. Biomaterials 24(27): 4921-4928.
32. Nicusor Fifere, Anton Airinei, Marius Dobromir, Liviu Sacarescu, Simona I Dunca, et al. (2021) Revealing the effect of synthesis conditions on the structural, optical, and antibacterial properties of cerium oxide nanoparticles. Nanomaterials 11(10): 2596.
33. Dale A Pelletier, Anil K Suresh, Gregory A Holton, Catherine K McKeown, Wei Wang, et al. (2010) Effects of engineered cerium oxide nanoparticles on bacterial growth and viability. Applied and environmental microbiology 76(24): 7981-7989.
34. Heiman F L Wertheim, Damian C Melles, Margreet C Vos, Willem van Leeuwen, Alex van Belkum, et al. (2005) The role of nasal carriage in Staphylococcus aureus infections. The Lancet infectious diseases 5(12): 751-762.
35. Mylotte JM, A Tayara, S Goodnough (2002) Epidemiology of bloodstream infection in nursing home residents: evaluation in a large cohort from multiple homes. Clinical infectious diseases 35(12): 1484-1490.
36. Jose Luis Lopez Miranda, Gustavo A Molina, Marlen Alexis González Reyna, Beatriz Liliana España Sánchez, Rodrigo Esparza, et al. (2023)

Antibacterial and anti-inflammatory properties of ZnO nanoparticles synthesized by a green method using sargassum extracts. International Journal of Molecular Sciences 24(2): 1474.

37. Khawla S Khashan, Ban A Badr, Ghassan M Sulaiman, Majid S Jabir, Sura A Hussain, et al. (2021) Antibacterial activity of Zinc Oxide nanostructured materials synthesis by laser ablation method. Journal of Physics: Conference Series.

38. Lalitha S Jairam, Dhanya Shri M, Akshatha Chandrashekar, T Niranjana Prabhu, Akshay Arjun, et al. (2024) Antibacterial and mechanical properties of cerium oxide nanoparticles modified glass ionomer cement. Materials Chemistry and Physics 315: 129040.

39. J Malleshappa, H Nagabhushana, S C Sharma, Y S Vidya, K S Anantharaju, et al. (2015) Leucas aspera mediated multifunctional CeO2 nanoparticles: structural, photoluminescent, photocatalytic and antibacterial properties. Spectrochimica Acta Part A: Molecular and Biomolecular Spectroscopy 149: 452-462.

40. Antoine Thill, Ophélie Zeyons, Olivier Spalla, Franck Chauvat, Jerôme Rose, et al. (2006) Cytotoxicity of CeO2 nanoparticles for Escherichia coli. Physico-chemical insight of the cytotoxicity mechanism. Environmental science & technology 40(19): 6151-6156.

41. Ophélie Zeyons, Antoine Thill, Franck Chauvat, Nicolas Menguy, Corinne Cassier-Chauvat, et al. (2009) Direct and indirect CeO2 nanoparticles toxicity for Escherichia coli and Synechocystis. Nanotoxicology 3(4): 284-295.

42. K Suresh Babu, M Anandkumar, T Y Tsai, T H Kao, B Stephen Inbaraj, et al. (2014) Cytotoxicity and antibacterial activity of gold-supported cerium oxide nanoparticles. International journal of nanomedicine 9: 5515-5531.

43. Soni B, S Makkar, S Biswas (2021) Defects induced tailored optical and magnetic properties of Zn- doped CeO2 nanoparticles synthesized by a facile sol-gel type process. Journal of Alloys and Compounds 879: 160149.

44. Ruixing Li, Shinryo Yabe, Mika Yamashita, Shigeyosi Momose, Sakae Yoshida, et al. (2002) UV-shielding properties of zinc oxide-doped ceria fine powders derived via soft solution chemical routes. Materials Chemistry and Physics 75(1-3): 39-44.

45. Aseena S, N Abraham, VS Babu (2023) Morphological and optical studies of zinc doped cerium oxide nanoparticles prepared by single step co-precipitation method. Materials Today: Proceedings 80: 1901-1905.

46. SA Hassanzadeh Tabrizi, Mehdi Mazaheri, M Aminzare, SK Sadrnezhaad (2010) Reverse precipitation synthesis and characterization of CeO2 nanopowder. Journal of Alloys and Compounds 491(1-2): 499-502.

47. Ponnar M, M Sathya, K Pushpanathan (2020) Enhanced UV emission and supercapacitor behavior of Zn doped CeO2 quantum dots. Chemical Physics Letters 761: 138087.

48. M A Majeed Khan, Wasi Khan, Maqusood Ahamed, Abdulaziz N Alhazaa (2017) Microstructural properties and enhanced photocatalytic performance of Zn doped CeO_2 nanocrystals. Scientific reports 7(1): 12560.